

Chemical potential beyond the quasiparticle mean fieldN. Dinh Dang^{1,2,*} and N. Quang Hung^{1,†}¹*Heavy-Ion Nuclear Physics Laboratory, RIKEN Nishina Center for Accelerator-Based Science, 2-1 Hirosawa, Wako City, 351-0198 Saitama, Japan*²*Institute for Nuclear Science and Technique, Hanoi, Vietnam*

(Received 15 September 2009; revised manuscript received 11 November 2009; published 4 March 2010)

The effects of quantal and thermal fluctuations beyond the BCS quasiparticle mean field on the chemical potential are studied within a model, which consists of N particles distributed amongst Ω doubly folded equidistant levels interacting via a pairing force with parameter G . The results obtained at zero and finite temperatures T within several approaches, which include the fluctuations beyond the BCS theory, are compared with the exact results. The chemical potential, defined as the Lagrangian multiplier to preserve the average number of particles, is compared with the corresponding quantity, which includes the effect from fluctuations of particle and quasiparticle numbers beyond the BCS quasiparticle mean field. The analysis of the results shows that the latter differs significantly from the former as functions of G and T . The chemical potential loses its physical meaning in the system with a fixed number of particles or after eliminating quantal fluctuations of particle (quasiparticle) numbers by means of particle number projection. The validity of the criterion for the signature of the transition to Bose-Einstein condensation, which occurs in infinite systems when the chemical potential hits the bottom of the energy spectrum, is reexamined for the finite multilevel model.

DOI: [10.1103/PhysRevC.81.034301](https://doi.org/10.1103/PhysRevC.81.034301)

PACS number(s): 21.60.Jz, 24.10.Pa, 24.60.Ky

I. INTRODUCTION

Fluctuations play an important role in small finite systems such as atomic nuclei. The mean-field theories, which work well for very large or infinite systems in condensed matter and solid state physics, need to be modified when applied to atomic nuclei, especially the light ones. Among these theories, the most popular one is the BCS theory, which describes the phenomenon of superconductivity (superfluidity). It is well known that this theory violates the particle number, which causes the quantal particle-number fluctuations (PNFs). At finite temperature ($T \neq 0$), the BCS theory also violates the unitarity relation $R^2 = R$ for the generalized single-particle density matrix R . It has been shown by Goodman [1] that this symmetry violation comes from the effects due to quasiparticle-number fluctuations (QNF), which are neglected within the Hartree-Fock-Bogoliubov (HFB) theory at $T \neq 0$. The PNF are of the quantal nature as they exist even at $T = 0$, whereas the QNF are thermal fluctuations because they arise only at $T \neq 0$.

The results of a considerable number of theoretical studies have shown that fluctuations in small systems indeed lead to significant modifications of quantities, which are defined within the mean field and/or thermal equilibrium, where the effects of fluctuations are ignored. Among the two unknowns, which are defined by solving the BCS equations, namely the pairing gap and chemical potential, much attention has been devoted so far to the study of the first one, the pairing gap. It has been shown, for instance, that removing quantal fluctuations by using various methods of particle-number projection (PNP) significantly improves the agreement between the theoretical

predictions and experimental data on pairing energies. The PNP also eliminates the shortcoming of the BCS theory, which breaks down at small values $G \leq G_c$ of the pairing interaction parameter, where the BCS equations have only trivial solutions [2–4]. At $T \neq 0$, the results of theoretical studies in the last three decades have also shown that thermal fluctuations smooth out the sharp transition between the superfluid phase to the normal one (the SN phase transition) in nuclei [5–10]. In very large or infinite systems, the SN phase transition takes place when the superfluid pairing gap $\Delta(T)$ collapses at a critical temperature $T_c \simeq 0.57\Delta(0)$, where $\Delta(0)$ is the value of the pairing gap at $T = 0$. However, in small systems such as nuclei, under the effects of thermal fluctuations, namely the QNF, the pairing gap never collapses, but decreases monotonously with increasing T .

The second quantity, the chemical potential, describes the change in energy when one particle is added to the system at constant entropy and volume. In nuclear physics, the vanishing of chemical potential indicates the vicinity of the nucleon drip line. In the study of Bose-Einstein condensation (BEC), as has been shown by Nozières and Schmitt-Rink (NSR) [11], one expects the system to undergo the BEC into a single quantum state with zero total momentum when the chemical potential of the bound pair of fermions reaches the bottom of the bound state band. The aim of the present article is to study the effects of quantal and thermal fluctuations on the chemical potential and some of their consequences within the exactly solvable multilevel pairing model, which is also called the ladder, picket-fence, or Richardson model.

The article is organized as follows. The chemical potential and its corresponding quantity, which includes the effects of fluctuations beyond the quasiparticle mean field are discussed in Sec. I. The numerical results obtained within the equidistant multilevel pairing model are analyzed in Sec. II. The last section summarizes the article, where conclusions are drawn.

* dang@riken.jp† On leave of absence from the Institute of Physics, Hanoi, Vietnam; nqhung@riken.jp

II. CHEMICAL POTENTIAL

The chemical potential has been first defined by Gibbs as the energy, which is required to add an infinitesimal quantity of a substance to any homogeneous mass, divided by the quantity of the substance added. This energy increase should not change the volume and entropy of the homogenous mass. Applied to the many-body systems, the chemical potential μ is the minimum energy required to add a particle to a system in thermal equilibrium with the heat bath. This condition requires that the grand potential $\Omega(\mu, T) \equiv F - \mu N$ of the system, whose average number of particles is equal to N , reaches the minimum, that is,

$$\delta\Omega(\mu, T) = \delta F - \mu\delta N = \delta\mathcal{E} - T\delta S - \mu\delta N = 0, \quad (1)$$

where $F = \mathcal{E} - TS$ is the Helmholtz free energy, \mathcal{E} is the total (internal) energy, S is the entropy, and T is the temperature of the system. From Eq. (1) it follows that the thermodynamic chemical potential μ of a system with the average number N of particles at a constant volume and temperature is given as

$$\mu = \frac{\partial F}{\partial N}. \quad (2)$$

In the case when the free energy F is a quadratic function of N , the definition Eq. (2) gives the same result as that obtained by using the arithmetic average,

$$\mu = \frac{1}{2}[\mu^{(+)} + \mu^{(-)}], \quad (3)$$

where $\mu^{(+)}$ and $\mu^{(-)}$ are the chemical potentials defined as half of the energy required to add two particles to a system with N and $N - 2$ particles, respectively,

$$\begin{aligned} \mu^{(+)} &= \frac{1}{2}[F(N + 2, \Omega) - F(N, \Omega)], \\ \mu^{(-)} &= \frac{1}{2}[F(N, \Omega) - F(N - 2, \Omega)], \end{aligned} \quad (4)$$

where Ω denotes the number of single-particle levels (the size of the system). This leads to

$$\mu = \frac{1}{4}[F(N + 2, \Omega) - F(N - 2, \Omega)]. \quad (5)$$

At $T = 0$, the entropy S vanishes, so that the free energy $F(N, \Omega)$ reduces to the ground-state energy $\mathcal{E}_{g.s.}(N, \Omega)$, and Eq. (5) turns to the conventional approximation for the chemical potential at zero temperature.

It is worth emphasizing that the concept of chemical potential μ is meaningful only in the presence of PNF. Therefore, at finite temperature, μ is defined within the grand canonical ensemble (GCE), where not only the energy, but also the particle number is allowed to fluctuate so that the variation over δN is possible. To get more insight into this issue we recall that an alternative quantity, which represents the effort of adding an extra particle to the system, is called the fugacity f , whose logarithm is equal to the thermodynamic chemical potential μ , that is,

$$\mu = T \ln f, \quad \text{or} \quad f = e^{\beta\mu}, \quad \beta = T^{-1}. \quad (6)$$

An average quantity, such as the energy \mathcal{E} , particle number N , and, consequently, the chemical potential μ itself, is calculated within the GCE as a weighted sum over systems with different numbers of particles. The weight is given by the grand partition

function $\mathcal{Z}(\beta, \mu)$. The latter is defined as

$$\mathcal{Z}(\beta, \mu) = \sum_{n=0}^{\infty} f^n Z_n(\beta), \quad Z_n(\beta) = e^{-\beta\mathcal{E}^{(n)}}, \quad (7)$$

where $Z_n(\beta)$ is the partition function of the canonical ensemble (CE) of the system with n particles. Indifferent of the GCE, within the CE only the energy is allowed to fluctuate whereas its particle number is fixed. The GCE becomes the CE if there is no PNF, that is, no summation takes place over the particle numbers at the right-hand side of Eq. (7). In this case, Eq. (7) reduces to $\mathcal{Z}_{n=N}(\beta, \mu) = f^N Z_N(\beta)$. Because at a fixed N , one should have $\mathcal{Z}_N(\beta, \mu) = Z_N(\beta)$, it follows that $f^N = 1$, or $\mu = 0$ within the CE. This argument shows that the chemical potential is a meaningful concept only within the GCE. Therefore, although the free energy F can be calculated exactly within the CE, where no PNF are allowed, the result for the chemical potential μ obtained from the definition Eq. (2) or the approximation Eq. (5) already involves several CEs with different numbers of particles, for example, $n = N$, and $N \pm 2$ in Eq. (5) (i.e., assuming the existence of PNF).

A. Within quasiparticle mean field

The present article considers the pairing Hamiltonian,

$$H = \sum_{jm} \epsilon_j a_{jm}^\dagger a_{jm} - G \sum_{jj'} \sum_{mm'>0} a_{jm}^\dagger a_{j\tilde{m}}^\dagger a_{j'm'} \tilde{a}_{j'm'}. \quad (8)$$

It describes a system of N particles with single-particle energies ϵ_j , generated by the particle creation operators a_{jm}^\dagger on j th orbitals with degeneracies $2\Omega_j$ ($\Omega_j = j + 1/2$), and interacting via a monopole-pairing force with the parameter G . The symbol $\tilde{}$ denotes the time-reversal operator, namely $a_{j\tilde{m}} = (-)^{j-m} a_{j-m}$. The eigenvalues and eigenvectors of this pairing Hamiltonian can be found by exact diagonalization [12]. The $d_s^{(n)}$ -degenerated eigenvalues $\mathcal{E}_s^{(n)}$, obtained for the system with n particles, are used to construct the grand partition function $\mathcal{Z}(\beta, \mu)$, which is employed to calculate the exact GCE total (internal) energy as [13]

$$\mathcal{E}_{\text{exact}} = \frac{1}{\mathcal{Z}(\beta, \mu)} \sum_{s,n} \mathcal{E}_s^{(n)} f^n Z_n(\beta), \quad Z_n(\beta) = \sum_s d_s^{(n)} e^{-\beta\mathcal{E}_s^{(n)}}. \quad (9)$$

The GCE sum in Eq. (9) is carried out over all $n = 1, \dots, \Omega-1$ with blocking properly taken into account for odd n . From the exact GCE total energy $\mathcal{E}_{\text{exact}}$, one calculates the entropy by using the Clausius definition, $\delta S = \beta\delta\mathcal{E}$, which leads to

$$S = \int_0^T \frac{1}{\tau} \frac{\partial \mathcal{E}}{\partial \tau} d\tau. \quad (10)$$

Consequently the free energy F is known, from which the exact μ can be estimated according to the definition Eq. (2) or approximation Eq. (5).¹

¹Notice that, when the grand partition function is known, one can use the differentials of $\ln \mathbf{Z}(\beta)_\alpha$ to obtain the entropy $S = \beta(\mathcal{E} - \mu N) + \ln \mathcal{Z}(\beta, \mu)$, which is equivalent to Eq. (10) (see Eqs. (2B-37a)–(2B-37c) in Ref. [14]). This expression is employed in the present article in

For a system with a given number N of particles such as an atomic nucleus, the chemical potential is often defined as a Lagrangian multiplier λ enforcing the constraint of density normalization, namely,

$$\delta \left\{ F[f_i] - \lambda \left(\sum_i f_i - N \right) \right\} = 0, \quad (11)$$

where f_i are the occupation numbers. This leads to the variational procedure,

$$(\delta F[f_i]/\delta f_i)|_{f_i=f_i^0} = \lambda, \quad (12)$$

where f_i^0 are the reference occupation numbers that minimize the energy. Definition Eq. (12) to determine the chemical potential λ is often used within the BCS-based approaches, where the single-particle mean field and the pairing correlations are unified into the quasiparticle mean field. The total energy \mathcal{E} and the particle-number constraint are calculated as the expectation values of the pairing Hamiltonian H (8) and particle-number operator \hat{N} , respectively, namely

$$\mathcal{E} = \langle H \rangle, \quad N = \langle \hat{N} \rangle, \quad (13)$$

where the symbol $\langle \dots \rangle$ denotes the average within the GCE at a given temperature $T \neq 0$. At $T = 0$ this GCE average is replaced with the expectation value in the ground state. The variational procedure is carried out within the quasiparticle representation \mathcal{H} of the Hamiltonian H , which is obtained by expressing the particle operators, a_j^\dagger and a_j , in the pairing Hamiltonian H [Eq. (8)] in terms of the quasiparticle ones, α_j^\dagger and α_j by using the canonical Bogoliubov transformation:

$$a_{jm}^\dagger = u_j \alpha_{jm}^\dagger + v_j \alpha_{j\bar{m}}, \quad a_{j\bar{m}} = u_j \alpha_{j\bar{m}} - v_j \alpha_{jm}^\dagger. \quad (14)$$

The explicit form of \mathcal{H} can be found in many references, for example, Eqs. (3)–(14) of Ref. [15]. The variational variables are the coefficients u_j and v_j , whereas the variation of the entropy over the quasiparticle occupation number n_j yields the explicit expression for n_j in the form of Fermi-Dirac distribution of noninteracting quasiparticles,

$$n_j = \frac{1}{e^{\beta E_j} + 1}, \quad (15)$$

with E_j being the quasiparticle energies. As the result of this variational procedure, the BCS equations are obtained, which determine the pairing gap Δ and the Lagrangian-multiplier chemical potential λ for a given single-particle spectrum with energies ϵ_j at a given value G , namely,

$$\Delta = \sum_j \Omega_j u_j v_j (1 - 2n_j), \quad (16)$$

$$N = 2 \sum_j \Omega_j [(1 - 2n_j)v_j^2 + n_j]. \quad (17)$$

calculations using the exact eigenvalues of the pairing Hamiltonian as it is free from errors caused by calculating numerically the derivative under the integration in Eq. (10).

The Bogoliubov's coefficients u_j and v_j have now the explicit form,

$$u_j^2 = \frac{1}{2} \left[1 + \frac{\epsilon'_j - \lambda}{E_j} \right], \quad v_j^2 = \frac{1}{2} \left[1 - \frac{\epsilon'_j - \lambda}{E_j} \right], \quad (18)$$

with the quasiparticle energies E_j and single-particle energies ϵ'_j , renormalized by the self-energy term $-Gv_j^2$,

$$E_j = \sqrt{(\epsilon'_j - \lambda)^2 + \Delta^2}, \quad \epsilon'_j = \epsilon_j - Gv_j^2. \quad (19)$$

B. Beyond quasiparticle mean field

Within the quasiparticle mean field, the two ways of calculating the chemical potential, either by using definition Eq. (2) for μ or as the Lagrangian multiplier λ from the variational Eq. (12), produce the same result (i.e., $\mu = \lambda$). However, it is well known that the BCS theory violates the particle number. The chemical potential λ found as the Lagrangian multiplier within the BCS theory ensures only the particle-number conservation in average [see Eq. (13)], just ignoring the effects caused by PNF,

$$\delta N^2 \equiv \langle \hat{N}^2 \rangle - N^2 \neq 0. \quad (20)$$

At $T \neq 0$, besides the quantal fluctuations of particle number, there appears the QNF as well,

$$\delta \mathcal{N}^2 \equiv \sum_j \delta \mathcal{N}_j^2 = \sum_j n_j (1 - n_j) \neq 0, \quad (21)$$

which are also neglected in the BCS theory at $T \neq 0$. The present section discusses the effects of these fluctuations on the chemical potential.

1. Effects of particle-number fluctuations within Lipkin-Nogami method

To eliminate the PNF, one has to carry out the PNP. The Lipkin-Nogami (LN) method [2] is a perspicacious approximate PNP before variation, which has been widely applied in calculations for realistic systems [16]. It proposes a variational procedure based on a trial Hamiltonian H_{LN} in the form,

$$H_{\text{LN}} = \mathcal{H} - \lambda_1 \hat{N} - \lambda_2 \hat{N}^2, \quad (22)$$

instead of $\mathcal{H} - \lambda \hat{N}$. As the result, the LN equations, obtained for the pairing gap and particle number, are formally the same as the BCS ones, Eqs. (16) and (17). However, the chemical potential λ is now replaced with its corresponding LN value, λ_{LN} ,

$$\lambda_{\text{LN}} = \lambda_1 + 2\lambda_2(N + 1), \quad (23)$$

whereas the LN renormalized single-particle energies,

$$(\epsilon'_j)_{\text{LN}} = \epsilon'_j + 4\lambda_2 v_j^2 = \epsilon_j + (4\lambda_2 - G)v_j^2, \quad (24)$$

replace the BCS values ϵ'_j given in Eqs. (18) and (19). It is obvious that λ_{LN} defined in Eq. (23) is no longer the same as the thermodynamic chemical potential μ_{LN} , because the latter,

according to the minimization Eq. (1) and definition Eq. (2), is equal to

$$\mu_{\text{LN}} = \frac{\delta F_{\text{LN}}}{\delta N} = \frac{\delta(\mathcal{E}_{\text{LN}} - TS)}{\delta N} = \lambda_1 + 2\lambda_2 N = \lambda_{\text{LN}} - 2\lambda_2. \quad (25)$$

The quantity λ_{LN} can be defined as the modified chemical potential beyond the BCS quasiparticle mean field to emphasize the fact that it takes into account the effects due to δN^2 , which is neglected within the BCS theory, although this definition should be taken with a grain of salt. Indeed, as the LN method is an approximate PNP, it partially restores the exact particle number (i.e., eliminating the PNF). An exact PNP would eventually conserve the particle number exactly, (i.e., it would eliminate completely the PNF). At $T \neq 0$, for example, the exact PNP would bring the GCE results back to the CE ones. In the latter case, the thermodynamic chemical potential μ becomes completely irrelevant as has been discussed previously. Therefore, strictly speaking, in the presence of PNF, only the quantity μ_{LN} , which neglects the effects due to δN^2 , preserves the full meaning of a true thermodynamical potential, not λ_{LN} .²

The total energy \mathcal{E}_{LN} is given as

$$\mathcal{E}_{\text{LN}} = \mathcal{E} - \lambda_2 \delta N^2. \quad (26)$$

The explicit expression of the PNF δN^2 is given by Eqs. (15)–(17) in Ref. [17], whereas \mathcal{E} has the same form as that obtained within the BCS theory. The parameter λ_2 is not a Lagrangian multiplier, but defined so that $\langle H_{\text{LN}} \hat{N}^2 \rangle_N = 0$. This leads to

$$\lambda_2^{(i)} = \frac{1}{2} \frac{\partial^2 \mathcal{E}^{(i-1)}}{\partial N^2}, \quad (27)$$

where the superscript i denotes the i th iteration, at which λ_2 converges to the desired accuracy. The explicit expression of λ_2 at finite T is given in Ref. [15]. At $T = 0$, the quasiparticle occupation numbers n_j vanish, so one recovers from Eqs. (16), (17), and (27) the zero-temperature LN equations, and the expression for λ_2 at $T = 0$ [2], respectively.

The trial Hamiltonian H_{LN} (22) is, in fact, the first order of the infinite expansion series,

$$H_\infty = \mathcal{H} - \sum_{j=1}^{\infty} \lambda_j N^j, \quad (28)$$

which contains all higher-order PNF such as $\delta N^j = \langle \hat{N}^j \rangle - N^j$ with $j > 2$ as well. By neglecting the effect of δN^j and taking the variation according to Eq. (1), this infinite series

²In a similar manner, the pairing gap is a mean-field concept with its true meaning only within the BCS theory. This gap collapses at a $T = T_c$ for $G > G_c$ or at any $G < G_c$. Meanwhile, the exact solutions of the pairing problem produce no pairing gap, but only pairing correlation energy, from which one can define the “exact” pairing gap. The latter, however, never collapses at any T and G . The approaches, which take into account thermal fluctuations beyond the quasiparticle mean field [5,6,8–10,18], also lead to the pairing gap that does not collapse at $T > T_c$, as has been discussed in Sec. I.

would eventually yield the new thermodynamic chemical potential μ_∞ in the form,

$$\mu_\infty = \lambda_1 + \sum_{j \geq 2}^{\infty} j \lambda_j N^{j-1}. \quad (29)$$

Similar to μ_{LN} , this thermodynamic chemical potential μ_∞ is different from $\lambda_\infty = \mu_\infty + 2\lambda_2 + \dots$, which is the quantity that includes all quantal effects due to PNF beyond the BCS quasiparticle mean field.

2. Effects of quasiparticle-number fluctuations within LN1+SCQRPA and MBCS theories

The effects of QNF are taken into account in a microscopic way within two recent approaches, called the modified BCS (MBCS) theory [9,10] and the Lipkin-Nogami plus self-consistent quasiparticle random-phase approximation (LN1+SCQRPA) [15]. Although both the LN1+SCQRPA and MBCS theories take the effects of QNF into account microscopically, they are based on different assumptions. The details of these approaches have been discussed thoroughly in Refs. [9,10,15,18], therefore, only the main results, necessary for the analysis in the present article, are summarized below.

(a) *LN1+SCQRPA*. The LN1+SCQRPA uses the same variational procedure as that employed for the derivation of the BCS and/or LN equations. However, it retains the expectation values of $\langle \mathcal{A}_j^\dagger \mathcal{A}_{j'}^\dagger \rangle$, $\langle \mathcal{A}_j^\dagger \mathcal{A}_{j'} \rangle$, and $\langle \mathcal{N}_j \mathcal{N}_{j'} \rangle$, with $\mathcal{A}_j^\dagger \equiv [\alpha_j^\dagger \otimes \alpha_j^\dagger]_0 / \sqrt{2}$ and $\mathcal{N}_j = \sum_m \alpha_{jm}^\dagger \alpha_{jm}$. These expectation values are neglected within the BCS and LN theories. As the result, within the LN1+SCQRPA one obtains a generalized level-dependent gap equation,

$$\Delta_j = \frac{G}{\langle \mathcal{D}_j \rangle} \sum_{j'} \Omega_{j'} \langle \mathcal{D}_j \mathcal{D}_{j'} \rangle u_j v_{j'}, \quad \mathcal{D}_j = 1 - \frac{\mathcal{N}_j}{\Omega_j}. \quad (30)$$

The expectation value of the product of two quasiparticle density operators at the right-hand side of Eq. (30) is calculated approximately by using the exact relation,

$$\langle \mathcal{D}_j \mathcal{D}_{j'} \rangle = \langle \mathcal{D}_j \rangle \langle \mathcal{D}_{j'} \rangle + \frac{\delta \mathcal{N}_{jj'}}{\Omega_j \Omega_{j'}},$$

with $\delta \mathcal{N}_{jj'} = \langle \mathcal{N}_j \mathcal{N}_{j'} \rangle - \langle \mathcal{N}_j \rangle \langle \mathcal{N}_{j'} \rangle,$ (31)

and the mean-field contraction,

$$\delta \mathcal{N}_{jj'} \simeq 2\Omega_j \delta \mathcal{N}_j^2 \delta_{jj'}, \quad \delta \mathcal{N}_j^2 \equiv n_j(1 - n_j), \quad (32)$$

with the quasiparticle occupation number n_j ,

$$n_j = \frac{\langle \mathcal{N}_j \rangle}{2\Omega_j} = \frac{1}{2}(1 - \langle \mathcal{D}_j \rangle). \quad (33)$$

As the result, the gap equation [Eq. (30)] is split to a sum of a quantal level-independent part, Δ , and a thermal level-dependent part, $\delta \Delta_j$, namely,

$$\Delta_j = \Delta + \delta \Delta_j, \quad (34)$$

where

$$\Delta = G \sum_{j'} \Omega_{j'} u_{j'} v_{j'} (1 - 2n_{j'}), \quad \delta\Delta_j = 2G \frac{\delta\mathcal{N}_j^2}{1 - 2n_j} u_j v_j. \quad (35)$$

The expression of the gap Δ_j differs from that of the BCS (LN) gap by the level-dependent part $\delta\Delta_j$, which contains the QNF $\delta\mathcal{N}_j^2$ on the j th orbital. The corrections due to coupling to the SCQRPA pair vibrations enter in the expression of the renormalized single-particle energies, which are now given as

$$(\epsilon'_j)_{\text{LN1+SCQRPA}} = \epsilon'_j + \frac{G}{\sqrt{\Omega_j}(1 - 2n_j)} \sum_{j'} \sqrt{\Omega_{j'}} (u_{j'}^2 - v_{j'}^2) \times (\langle \mathcal{A}_j^\dagger \mathcal{A}_{j' \neq j}^\dagger \rangle + \langle \mathcal{A}_j^\dagger \mathcal{A}_{j'} \rangle), \quad (36)$$

where the expectation values $\langle \mathcal{A}_j^\dagger \mathcal{A}_{j'}^\dagger \rangle$ and $\langle \mathcal{A}_j^\dagger \mathcal{A}_{j'} \rangle$ are calculated in terms of the QRPA forward- and backward-going amplitudes X and Y , as well as the occupation numbers of the QRPA phonons. The approximate PNP is carried out within the LN method in the same way as has been discussed in the previous section. The quasiparticle occupation numbers n_j are also calculated taking into account the effects of coupling to the QRPA vibrations, therefore, different from the Fermi-Dirac distribution Eq. (15) of noninteracting fermions. The resulting equations form a closed set of the LN1+SCQRPA equations, which are solved self-consistently by iteration.

(b) *MBCS*. The HFB theory at $T \neq 0$, and its limit, the BCS theory, violate the unitarity relation $R^2 = R$ for the generalized single-particle density matrix R . It has been pointed out in Ref. [1] that the source of this violation is the effects due to QNF, which are neglected within the HFB and BCS theories, because $\text{Tr}[R(T)^2 - R(T)] = 2\delta\mathcal{N}^2 \neq 0$, which is twice the QNF. The MBCS theory takes into account the effects of QNF by means of the secondary Bogoliubov transformation from the quasiparticle operators, α_{jm}^\dagger and α_{jm} , to the modified quasiparticle ones, $\bar{\alpha}_{jm}^\dagger$ and $\bar{\alpha}_{jm}$,

$$\begin{aligned} \bar{\alpha}_{jm}^\dagger &= \sqrt{1 - n_j} \alpha_{jm}^\dagger + \sqrt{n_j} \alpha_{j\bar{m}}, \\ \bar{\alpha}_{j\bar{m}} &= \sqrt{1 - n_j} \alpha_{j\bar{m}} - \sqrt{n_j} \alpha_{jm}^\dagger, \end{aligned} \quad (37)$$

where the quasiparticle occupation numbers n_j are approximated by the Fermi-Dirac distribution (15). It was shown in Sec. III A of Ref. [10] that this secondary Bogoliubov transformation eventually restores the unitarity relation for the modified quasiparticle space. As the result of transformation [Eq. (38)] the MBCS equations for the pairing gap and particle number are obtained in the form,

$$\bar{\Delta} = \Delta + \delta\Delta, \quad \Delta = G \sum_j \Omega_j u_j v_j (1 - 2n_j), \quad (38)$$

$$\delta\Delta = G \sum_j \Omega_j (v_j^2 - u_j^2) \delta\mathcal{N}_j,$$

$$N = 2 \sum_j \Omega_j [(1 - 2n_j)v_j^2 + n_j - 2u_j v_j \delta\mathcal{N}_j]. \quad (39)$$

Similar to the LN1+SCQRPA, the MBCS gap [Eq. (38)] also consists of a quantal part, Δ , which is formally identical to

the BCS gap, and a thermal part, $\delta\Delta$, which contains the QNF. But, different from the LN1+SCQRPA gap, the MBCS gap is level independent with a different functional form of the thermal gap $\delta\Delta$. Moreover, because the QNF also affect the single-particle density via the last term at the right-hand side of the number equation [Eq. (39)], the chemical potential λ also changes with T within the MBCS theory and differs from that obtained within the BCS and LN theories.

C. Application in the study of BCS-BEC transition

The chemical potential μ has been employed in Ref. [11] to identify the onset of BEC in an attractive fermion gas. Applying the same concept to the finite systems with discrete single-particle levels, it is also true that, if the interaction is sufficiently strong, two fermions form a singlet bound pair, whose minimum energy is ϵ_b with $-\epsilon_b$ being the binding energy. The internal wave function ϕ_j of the pair creation extends over a characteristic distance $\sim \epsilon_b^{-1/2}$. If two bound pairs have only a small overlap ($|\phi_j| \ll 1$), they can be treated as a gas of structureless bosons. When this happens within the BCS theory, this means

$$\phi_j \equiv \frac{\Delta}{\sqrt{(\epsilon_j - \lambda)^2 + \Delta^2}} \ll 1, \quad (40)$$

and the BCS gap equation reduces, in leading order, to the Schrödinger equation for a single bound pair, whose eigenvalue is the pair chemical potential $\mu_P \equiv 2\mu$. Its zeroth order yields $2\mu = \epsilon_b$, as for an ideal Bose gas [11]. Therefore, in the same way as has been carried out in Ref. [11], the smooth BCS-BEC transition into a single quantum state with zero total momentum at $T = 0$ takes place if the positive pair chemical potential μ_P monotonously decreases with increasing G and eventually reaches the bottom of the bound pair spectrum, $\epsilon_b = 2\epsilon_1$, at a certain value $G = G_c^{\text{BEC}}$, higher than which ($G > G_c^{\text{BEC}}$) μ_P continues to decrease. If the bottom of the single-particle spectrum ϵ_1 is chosen to be equal to zero, this means $\mu_P = 0$ or $\mu = 0$ at $G = G_c^{\text{BEC}}$, and becomes negative at $G > G_c^{\text{BEC}}$. The choice of the positive single-particle energies with the bottom of the spectrum located at zero in the present pairing model is not simply a matter of an energy shift, but reflects a real physical situation. Indeed, if there are only two particles in the model, they will form a bound state for a finite value G of the attractive pairing interaction because the lowest eigenvalue of the diagonalization is below the lowest level. By putting only four, or six, etc. particles in the Ω -level system, a bound state of these four, or six, etc. particles will always have a negative energy (i.e., below the lowest level). In this way, even the neutron matter could become bound, if the nucleon-nucleon attractive interaction was sufficiently strong. As the number of particles increases, the Fermi surface starts to build up with a positive value for μ depending on the value of G . Within the BCS-based approaches, for example, the chemical potential μ goes from a negative value (i.e., the one for the bound state), to a positive one (i.e., that for an unbound state) as the interaction strength G decreases. In the present article, we consider the opposite direction, namely, the increase of the pairing interaction G , which causes the

decrease of the chemical potential, determined as positive at $G = 0$ within the application to the BCS-BEC transition.

III. RESULTS OF NUMERICAL CALCULATIONS

The Richardson model used in numerical calculations consists of Ω doubly folded equidistant levels, which interact via the pairing force with parameter G . The level distance is chosen equal to 1 MeV. In the absence of the interaction, the lowest $N/2$ levels are filled with N particles (two particles on each level). The case with $N = \Omega$ is called half-filled, whereas those with $N < \Omega$ and $N > \Omega$ are called underfilled and overfilled, respectively.

A. Chemical potentials within and beyond quasiparticle mean field at $T = 0$

In the present and next sections we consider the single-particle energies counted from the highest occupied Hartree-Fock level, namely,

$$\epsilon_j = j - \frac{1}{2}(N + 1), \quad j = 1, \dots, \Omega. \quad (41)$$

With this choice of single-particle energies, the exact value of the chemical potential μ for the half-filled case ($\Omega = N$) is independent of T and N , and equal to $-G/2$, which is the same as the BCS chemical potential λ at $G > G_c$. This can be easily checked by using a Ω -folded degenerated two-level model [19], where one finds $G_c = 1/(2\Omega - 1)$.

On the contrary, once the effects of PNF are taken into account, the chemical potential (or rather, parameter) λ_{LN} , which is obtained from Eq. (23) and shown as a dashed line in Fig. 1, deviates from its quasiparticle mean-field value $-G/2$ already at $G = 0$ because the quantity $\alpha \equiv 4\lambda_2 - G \neq 0$ even at $G = 0$ (or $\lambda_2 \neq 0$ even at $\Delta = 0$). This deviation increases with G . As has been analyzed in Ref. [2], this discrepancy is caused by the admixture of the four-quasiparticle components in the ground state from the omission of the term $\sim(\alpha^\dagger)^4$ of the trial Hamiltonian. Consequently, the energy shift $\Delta\mathcal{E}_{LN}$ of the ground state obtained within the LN method at very small G does not coincide with the prediction by the perturbation theory. However, this discrepancy vanishes after adding the four-quasiparticle contribution to $\Delta\mathcal{E}_{LN}$.

We also calculated the exact values of parameters λ_2 from Eq. (27), and λ_1 from Eq. (25) by using the exact free energy F_{LN} , which is obtained from the exact \mathcal{E}_{LN} given by Eq. (26) with the entropy equal to zero at $T = 0$. From them the exact λ_{LN} is found by using Eq. (23). These exact values (solid lines in Fig. 1) practically coincide with those obtained by solving the LN equations. These results demonstrate how the chemical potential μ is different from its corresponding quantity, which included the effects due to quantal fluctuations beyond the quasiparticle mean field.

B. Chemical potentials within and beyond quasiparticle mean field at $T \neq 0$

The chemical potential μ of the Richardson model (equal to λ in the quasiparticle mean field) becomes a constant, which remains in the middle of the single-particle spectrum (i.e., zero in the present choice of ϵ_j) only in the half-filled case

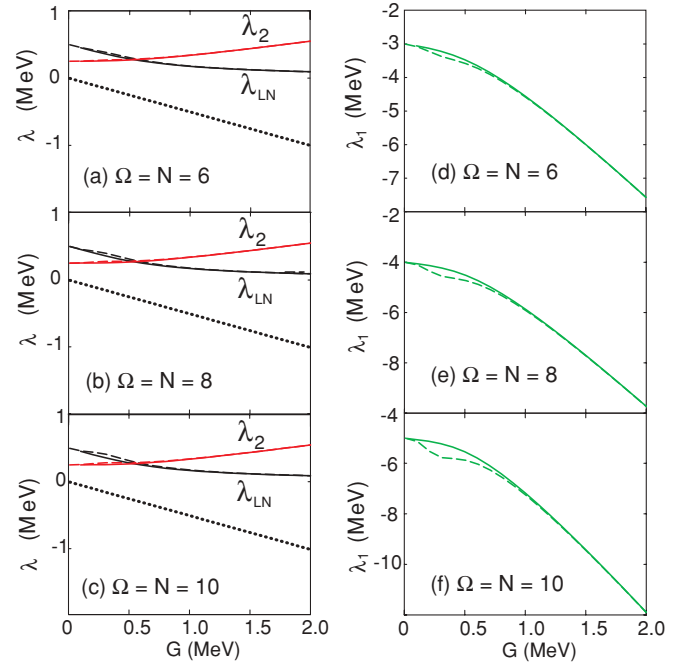


FIG. 1. (Color online) Chemical potential λ_{LN} , the parameters λ_2 [(a)–(c)], and λ_1 [(d)–(f)] as functions of pairing interaction parameter G at $T = 0$ for $\Omega = N = 6, 8$, and 10 . The solid and dashed lines are the exact and LN results, respectively, whereas the dotted lines show the $-G/2$ values.

that neglects the self-energy corrections $-Gv_j^2$ in the single-particle energies ϵ'_j (19). In all other cases, where $\Omega \neq N$, the chemical potential μ depends on temperature T , no matter the self-energy corrections $-Gv_j^2$ are included or not. The values of μ obtained within the BCS theory are shown in Fig. 2 as functions of T for the underfilled cases with $\Omega = 11, N = 10$, at $G = 0.4$ MeV, and $\Omega = 12, N = 8$, at $G = 0.6$ MeV along with the exact GCE and CE results. To be compared with the BCS results obtained without the self-energy corrections, the exact GCE (CE) results are calculated by using the exact GCE (CE) total energy shifted by $-G \sum_j f_j^2$, where f_j are the exact single-particle occupation numbers obtained within the GCE (CE) (see the thin solid lines in Fig. 2). The BCS chemical

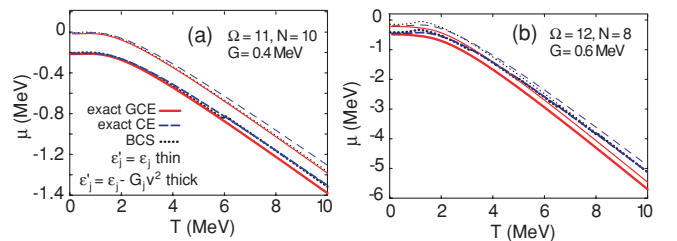


FIG. 2. (Color online) Chemical potentials as functions of temperature T for the underfilled cases with $\Omega = 11, N = 10$ (a) and $\Omega = 12, N = 8$ (b). The dotted, solid, and dashed lines are the BCS, exact GCE, and CE results, respectively. The thin lines denote the BCS results obtained without the self-energy corrections $-Gv_j^2$ in the single-particle energies, whereas the thick lines stand for the results obtained including the self-energy correction terms.

potentials decrease with increasing T at $T > T_c$ in agreement with the exact GCE and CE results [Eq. (2)]. Neglecting the self-energy corrections causes only a shift upward of around $0.2 \sim 0.3$ MeV. However, the BCS results, obtained including the self-energy corrections $-Gv_j^2$, contain some small jumps at the values of T where the chemical potential crosses the single-particle levels. These singularities lead to some small fluctuations in the values μ obtained in the approximations beyond the mean field such as the LN1+SCQRPA considered in the present article, and also leads to a slower convergence. For the case with $\Omega = N + 1 = 11$, which we choose as an illustration below, there is no qualitative difference between the results obtained with and without the self-energy corrections up to $T = 6$ MeV [see Fig. 2(a)]. Therefore, the terms $-Gv_j^2$ will be omitted in further calculations at $T \neq 0$ for simplicity.

The free energies obtained for the systems with $\Omega = N + 1 = 11$ at $G = 0.4$ MeV and $\Omega = N = 50$ at $G = 0.3$ MeV are shown in Figs. 3(a) and 3(c) as functions of T . They all show the general trend of decreasing with increasing T . At $T \leq T_c$ the LN1+SCQRPA offers the lowest value for the free energy, which is the closest to the exact one for $\Omega = N + 1 = 11$. However, at high T , where the quantal fluctuations vanish, and the thermal fluctuations become important, the MBCS free energies turn out to be the lowest ones. In the case with $\Omega = N + 1 = 11$, the MBCS and exact results coincide at $T \geq 1.7$ MeV.

Regarding the chemical potentials, one finds a clear difference between λ and μ [Eq. (2)] as functions of T as well. The thermodynamic potential μ starts from zero and decreases with increasing T in the underfilled case [Fig. 3(b)],

whereas it remains temperature independent in the half-filled case with $\Omega = N$ [Fig. 3(d)]. The MBCS result with $\Omega = 11$ and $N = 10$ exhibits a μ , which slightly increases at $T \sim 1$ MeV. The reason is due to the shortcoming of the MBCS theory at low Ω and N , which has been discussed in a series of articles [9,10,20], and we are not going to repeat it here. Therefore, when μ is calculated within the MBCS theory by using Eq. (2) for $\Omega = 11$ and $N = 10$, the result can be obtained only up to $T \sim 1$ MeV. The chemical potential λ that includes the effects of quantal and/or thermal fluctuations beyond the quasiparticle mean field, on the contrary, is quite different from μ . The LN and LN1+SCQRPA values for λ are significantly larger than zero, and decrease with increasing T to merge with μ only at $T > T_c$. The ‘‘exact’’ λ_{LN} is calculated by using the same Eq. (23), where λ_2 is given by Eq. (27) with the exact energy \mathcal{E} , whereas λ_1 is found from Eq. (25) with the exact \mathcal{E}_{LN} from Eq. (26) and exact S given by Eq. (10). This exact λ_{LN} is shown as the thin solid line in Fig. 3(b), which decreases smoothly as T increases, and crosses zero only at $T \sim 4$ MeV. The values of λ obtained within the MBCS theory show a different temperature dependence. It is zero at $T = 0$ because PNP is not included in the MBCS theory. As T increases, the MBCS λ increases sharply up to T_c , then it continues to increase (decrease) slightly with T in the case of small (large) Ω [see Figs. 3(b) and 3(d)]. Similar to the chemical potential λ_{LN} defined beyond the BCS quasiparticle mean field, the quantity λ obtained by solving the MBCS equations loses its meaning as the thermodynamic chemical potential μ because it includes the effects due to QNF. In this sense, within the MBCS theory, only the quantity μ , which is shown as the thick dash lines in Figs. 3(b) and 3(d), corresponds to a strict thermodynamic chemical potential.

C. Chemical potentials and the onset of BEC in finite systems

Following the discussion in Sec. II C for the numerical calculations regarding the BCS-BEC transition, we choose the single-particle energies $\epsilon_j = j - 1$ with $j = 1, \dots, \Omega$ (MeV), that is, all the levels have positive energies, except the lowest one, $\epsilon_1 = 0$, with both N and Ω being even numbers ($N \leq 2\Omega$). At small N and Ω , the mean-field chemical potential λ can increase or decrease with increasing G depending on whether the model is overfilled ($N > \Omega$), half-filled ($N = \Omega$), or underfilled ($N < \Omega$). This can be easily seen

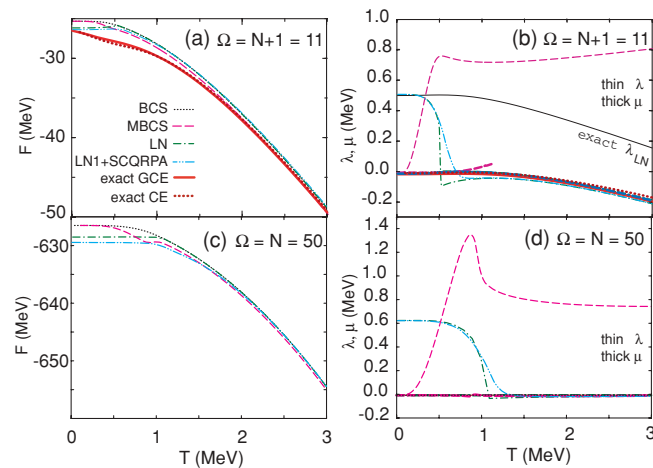


FIG. 3. (Color online) Free energies F and chemical potentials μ and λ as functions of temperature T for $\Omega = N + 1 = 11$ at $G = 0.4$ MeV (a,b) and $\Omega = N = 50$ (c,d) at $G = 0.3$ MeV. In (a) and (c) the thin dotted, dash-dotted, and dash-double dotted lines are the BCS, LN, and LN1+SCQRPA results, respectively. The MBCS results are shown by the dashed lines, whereas the thick solid and thick dotted lines in (a) are the exact free energy within the GCE and CE, respectively. In (b) and (d), except for the thin solid line representing the exact λ_{LN} as explained in the text, the other thin lines show the chemical potentials λ obtained within the above-mentioned approximations as notated in (a) and (c), whereas the thick lines are the corresponding thermodynamic chemical potentials μ .

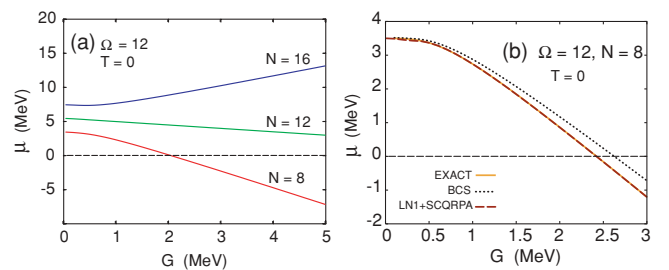


FIG. 4. (Color online) (a) Chemical potential μ within the BCS theory as a function of G for $\Omega = 12$ and $N = 8, 12$, and 16 . (b) Chemical potential as a function of G for the underfilled system with $\Omega = 12$ and $N = 8$. The dotted, dashed, and solid lines are the BCS, LN1+SCQRPA, and exact results, respectively.

in the simplest illustration using the seniority model with one single 2Ω -folded level, whose eigenvalue is given as a function of seniority s as [21]

$$\mathcal{E}_s(N, \Omega) = -\frac{G\Omega}{4} \left[\frac{s^2}{\Omega} - 2(s - N) \left(1 + \frac{1}{\Omega} \right) - \frac{N^2}{\Omega} \right]. \quad (42)$$

The chemical potential $\mu_{\text{sen.}}(T = 0)$ at $T = 0$, according to Eq. (2), is

$$\mu_{s=0}(T = 0) = \frac{\partial \mathcal{E}_{s=0}(N, \Omega)}{\partial N} = -\frac{G}{2}(\Omega - N + 1). \quad (43)$$

This result for μ , which is obtained as the derivative of the free energy (or total energy at $T = 0$) over the particle number N , is the same as the prediction by the approximation Eq. (5) because $\mathcal{E}_s(N, \Omega)$ is a quadratic function of N in the present case, whereas $S(T = 0) = 0$. This chemical potential is negative if $N \leq \Omega$, and positive if $N > \Omega$ because both N and Ω are even. Consequently, as G increases, the chemical potential will decrease in the underfilled and half-filled cases, and increase in the overfilled case. The physics here is related to the behavior of the pairing gap in a small shell, which is equal to $\Delta = G\sqrt{N(\Omega - N/2)/2}$ [21]. This gap is zero for the empty ($N = 0$) and completely filled shells ($N = 2\Omega$), and maximum when the shell is half-filled ($N = \Omega$). If the configuration space Ω is very large or infinite, whereas N is small, the model is always strongly underfilled ($N \ll \Omega$), so the chemical potential always decreases with increasing G . This is the situation of infinite-size systems because the upper limit of k in the kinetic energy $k^2/2m$ is very high or infinite, whereas the number of particles is finite. In the opposite case, if the model is overfilled ($N > \Omega$), we can never get BEC (i.e., structureless bosons from the pairs of fermions) by increasing the coupling strength G because the chemical potential will never reach the bottom of the spectrum, being always increasing with G . This observation is confirmed by the results for the chemical potential μ , which are obtained within the multilevel model with $\Omega = 12$ and $N = 8, 12$, and 16 ,

and displayed in Fig. 4(a). This figure shows that μ decreases with increasing G only for $N \leq \Omega$, and the stronger the model is underfilled, the steeper the decrease of μ one gets as G increases. The chemical potential μ is a smooth function of G , as Figs. 4(a) and 4(b) demonstrate. Moreover, the results displayed in Fig. 4(b) show that the LN1+SCQRPA and exact results coincide, and μ crosses zero at $G_c^{\text{BEC}} \simeq 2.4$ MeV, signaling the appearance of the BEC as a single quantum state. The BCS prediction slightly overestimates the exact and LN1+SCQRPA results, crossing zero at $G_c^{\text{BEC}} \simeq 2.65$ MeV.

As has been mentioned in Sec. II C, a negative value of μ is considered as the signature of the BCS-BEC transition in infinite systems. We have shown above that a similar behavior of μ also takes place in the finite underfilled system at large G . However, whether this still remains the signature of the BCS-BEC transition in finite systems is not straightforward. In Fig. 5, we show the ground-state energies (at $T = 0$) and the total energies (at $T \neq 0$) as functions of the particle number N at $G = 10$ MeV. It is seen from this figure that, in the strong coupling regime, the multilevel model under consideration becomes very similar to the seniority model, in the sense that the level distance can be neglected in first-order approximation. From Eq. (42) it follows that only at $N \ll \Omega$ (i.e., the low-density limit or diluted systems), the binding energy of the ground state (i.e., the ground-state energy of the system taken with the reverse sign) approaches the limit equal to the binding energy of just one pair multiplied by the number $N_p = N/2$ of pairs. In this limit, the condensate of $N/2$ noninteracting fermion pairs, whose binding energy is $G\Omega$ per pair, becomes a condensation of $N_B = N/2$ bosons (i.e., a BEC). This trend can be clearly seen in Figs. 5(a) and 5(b), which shows that, as the ratio N/Ω decreases on one hand, and Ω increases on the other hand, the BCS, LN1+SCQRPA, and exact ground-state energies become closer to the BEC limit. We also notice that the LN1+SCQRPA results practically coalesce with the exact ones at all N . At $T \leq T_c/2$ the pairing gap decreases only slightly as compared with the gap at $T = 0$, so the picture remains nearly the same for the total

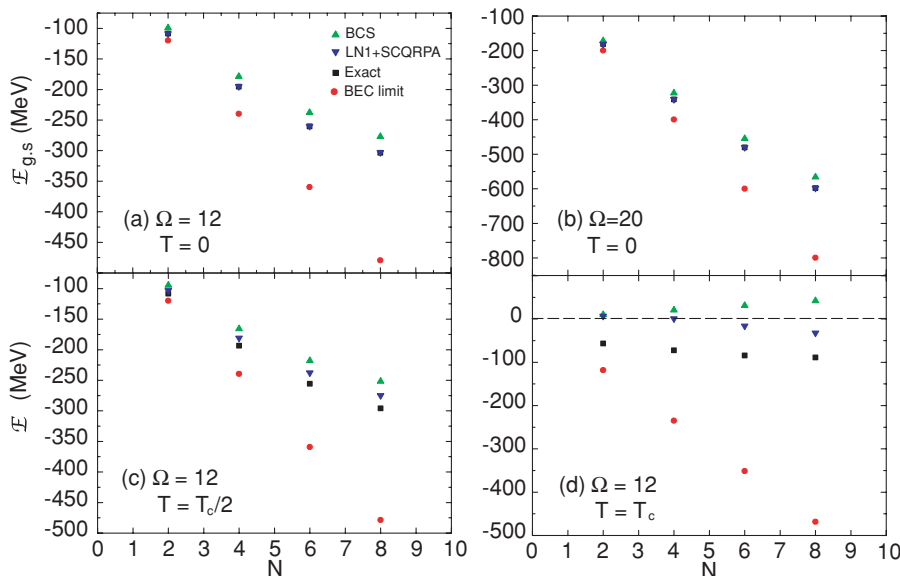


FIG. 5. (Color online) (a) Ground-state energies versus the particle number N for $\Omega = 10$ at $G = 10$ MeV. (b) The same as (a) for $\Omega = 20$. (c) Total energies versus N for $\Omega = 12$ at $G = 10$ MeV at $T = T_c^{\text{BCS}}/2$. (d) The same as (c) at $T = T_c^{\text{BCS}}$. The notations for the results are shown in the figure.

energies up to $T \simeq T_c/2$ [see Fig. 5(c)]. However, at $T \geq T_c$, where the BCS gap vanishes whereas the LN1+SCQRPA and exact gaps become rather small, the total energies strongly deviate from the BEC limit. As shown in Fig. 5(d), the total energies predicted by the exact results and the LN1+SCQRPA theory at $T = T_c$ are much larger than the BEC limit, especially at larger N , whereas the total energy predicted by the BCS theory even turns positive at $N \geq 4$. Meanwhile, the total energy in the BEC limit increases only slightly by 10 MeV at $N = 8$.³ This example demonstrates that, even if the system reaches the BEC in the strong coupling regime at $T = 0$, increasing T destroys the superfluid pairing correlations. As the result, at $T \geq T_c$ even the lightest system can no longer stay in the BEC regime.

IV. CONCLUSIONS

The present article studies the effects due to quantal and thermal fluctuations beyond the BCS quasiparticle mean field on the chemical potential within a model, which consists of N particles distributed amongst Ω doubly folded equidistant levels interacting via a pairing force with parameter G . The results obtained at zero and finite temperatures T within several approaches such as the BCS, LN, LN1+SCQRPA, and MBCS theories are compared with the exact results, whenever the latter are available. The analysis of the numerical results show that, in general, the chemical potential of the equidistant multilevel pairing model depends on the parameter

³The results obtained within the BCS and LN1+SCQRPA theories including the self-energy term in the single-particle energies, and the exact results obtained without subtracting the corresponding term $-G \sum_k f_k^2$ are only slightly smaller than those shown in Fig. 5. The largest difference, seen at $N = 8$, does not exceed 5%.

of the pairing interaction and temperature. It remains a constant in the middle of the spectrum only in the half-filled case within the mean-field approximation that neglects the self-energy corrections to the single-particle energies. Beyond the quasiparticle mean field, quantal and thermal fluctuations significantly alter the chemical potential as a function of G and/or T . As the result, the quantity that corresponds to the chemical potential but includes the effects due to PNF or QNF, such as the parameter λ_{LN} within the LN method or λ within the MBCS theory, gradually loses its strict physical meaning as a chemical potential with increasing T , and as the approximate PNP approach the exact one, where all PNPs are eliminated.

In the study of the chemical potential as a measure to search for the onset of BCS-BEC transition in finite systems, we have shown that the system in the strong coupling regime can approach the BEC limit only in the strongly underfilled case (when the number N of particles is much smaller than the size, that is, number Ω of the levels of the system) at zero temperature. Even if it can take place, increasing temperature will drive the system out of the BEC limit. However, this is a conclusion obtained here within a simple one-dimensional model. How this feature is modified in realistic nuclei remains a question to be answered in the future studies.

ACKNOWLEDGMENTS

The authors thank Peter Schuck (IPN Orsay) for proposing the application to BCS-BEC transition and fruitful discussions. The numerical calculations were carried out using the FORTRAN IMSL Library by Visual Numerics on the RIKEN Integrated Combined Cluster (RICC) system. N.Q.H. acknowledges support from the Nishina Memorial program at RIKEN Nishina Center. He also thanks the Vietnam National Foundation for Science and Technology Development (NAFOSTED) for support through Grant No. 103.04.54.09, under which a part of this work was carried out.

- [1] A. L. Goodman, Phys. Rev. C **29**, 1887 (1984).
- [2] H. J. Lipkin, Ann. Phys. **9**, 272 (1960); Y. Nogami, Phys. Rev. **134**, B313 (1964); H. C. Pradhan, Y. Nogami, and J. Law, Nucl. Phys. **A201**, 357 (1973); J. F. Goodfellow and Y. Nogami, Can. J. Phys. **44**, 1321 (1966).
- [3] H. Olofsson, R. Bengtsson, and P. Möller, Nucl. Phys. **A784**, 104 (2007).
- [4] N. Q. Hung and N. D. Dang, Phys. Rev. C **76**, 054302 (2007).
- [5] L. G. Moretto, Nucl. Phys. **A182**, 641 (1972).
- [6] A. L. Goodman, Phys. Rev. C **29**, 1887 (1984).
- [7] N. Dinh Dang and N. Zuy Thang, J. Phys. G **14**, 1471 (1988).
- [8] N. D. Dang, P. Ring, and R. Rossignoli, Phys. Rev. C **47**, 606 (1993); R. Rossignoli, P. Ring, and N. D. Dang, Phys. Lett. **B297**, 9 (1992).
- [9] N. Dinh Dang and V. Zelevinsky, Phys. Rev. C **64**, 064319 (2001); **65**, 069903(E) (2002); N. Dinh Dang and A. Arima, *ibid.* **67**, 014304, (2003); **68**, 039902(E) (2003); N. D. Dang and A. Arima, *ibid.* **74**, 059801 (2006); N. Dinh Dang, Nucl. Phys. **A784**, 147 (2007); N. D. Dang, Phys. Rev. C **76**, 064320 (2007).
- [10] N. D. Dang and A. Arima, Phys. Rev. C **68**, 014318 (2003).
- [11] P. Nozières and S. Schmitt-Rink, J. Low Temp. Phys. **59**, 195 (1985).
- [12] A. Volya, B. A. Brown, and V. Zelevinsky, Phys. Lett. **B509**, 37 (2001).
- [13] N. Q. Hung and N. D. Dang, Phys. Rev. C **79**, 054328 (2009).
- [14] A. Bohr and B. Mottelson, *Nuclear Structure*, Vol. 1 (Benjamin, New York, 1969).
- [15] N. Dinh Dang and N. Quang Hung, Phys. Rev. C **77**, 064315 (2008).
- [16] P.-G. Reinhard, W. Nazarewicz, M. Bender, and J. A. Maruhn, Phys. Rev. C **53**, 2776 (1996); T. R. Rodriguez, J. L. Egido, and L. M. Robledo, *ibid.* **72**, 064303 (2005); M. V. Stoitsov, J. Dobaczewski, R. Kirchner, W. Nazarewicz, and J. Terasaki, *ibid.* **76**, 014308 (2007); G. F. Bertsch, C. A. Bertulani, W. Nazarewicz, N. Schunck, and M. V. Stoitsov, *ibid.* **79**, 034306 (2009).
- [17] N. Dinh Dang, Z. Phys. A **335**, 253 (1990).
- [18] N. Q. Hung and N. D. Dang, Phys. Rev. C **78**, 064315 (2008).
- [19] N. Dinh Dang, Eur. Phys. A **16**, 181 (2003).
- [20] V. Yu. Ponomarev and A. I. Vdovin, Phys. Rev. C **72**, 034309 (2005); **74**, 059802 (2006)
- [21] P. Ring and P. Schuck, *The Nuclear Many-Body Problem* (Springer, Heidelberg, 2004).